Incomitant Strabismus Associated with Instability of Rectus Pulleys

Sei Yeul Oh,[1,2] *Robert A. Clark,*[1,3] *Federico Velez,*[1] *Arthur L. Rosenbaum,*[1] *and Joseph L. Demer*[1,4]

Purpose. Connective tissue pulleys serve as functional mechanical origins of the extraocular muscles (EOMs) and are normally stable relative to the orbit during gaze shifts. This study evaluated pulley stability in incomitant strabismus.

Methods. Contiguous 2- or 3-mm thick magnetic resonance images (MRIs) perpendicular to the orbital axis spanned the anteroposterior extents of 12 orbits of six patients with incomitant strabismus. Imaging was performed in central gaze, supraduction, infraduction, abduction, and adduction. Rectus EOM paths were defined by their area centroids and plotted in a normalized, oculocentric coordinate system. Paths of EOMs ran toward the pulleys. Sharp EOM path inflections in secondary gaze indicated pulley locations in three dimensions.

Results. MRI revealed substantial inferior shift of the lateral rectus (LR) pulley of up to 1 mm during vertical gaze shifts in patients with axial high myopia and a posterior shift from abduction to adduction in simulated Brown syndrome. There was substantial LR pulley shift opposite the direction of vertical gaze in a subject with X-pattern exotropia who had undergone repeated LR surgery. The medial rectus (MR) pulley shifted inferiorly with gaze elevation in Marfan syndrome. Pulley instability was associated with significantly increased globe translation during gaze shifts.

Conclusions. Pulley instability, resulting in EOM sideslip during ductions, occurs in some cases of incomitant strabismus. Resultant patterns of strabismus may depend on static pulley positions, pulley instability, and coexisting globe translation that alters pulley locations relative to the globe. Translational instability of pulleys and the globe could produce abnormalities in actions of otherwise normal EOMs, and connective tissue disorders causing these instabilities should be considered as potential causes of strabismus. (*Invest Ophthalmol Vis Sci.* 2002;43:2169–2178)

Annular condensations of the connective tissue sleeves of the posterior Tenon capsule, composed of collagen and elastin stiffened by smooth muscle, envelope the rectus extraocular muscles (EOMs) and are firmly anchored to each other and to the orbital walls.[1–3] High-resolution magnetic resonance imaging (MRI) in alert subjects has demonstrated that these tissue sleeves function as pulleys for the rectus EOMs, minimizing sideslip relative to the orbit of posterior EOM paths during globe rotation and determining the effective pulling direction of each EOM.[4–6] The mechanical action of a pulley in stabilizing the EOM's path relative to the orbit causes a transverse path inflection in secondary and tertiary gaze positions. Anteriorly, between the insertion and the pulley, the EOM and its tendon would have to move to follow the insertion on the rotating eye. At the functional pulley and posteriorly, the EOM path would shift only as permitted by elasticity of the pulley suspension. The inflection between the stable posterior path and moving anterior path is thought to define the location of the pulley in three dimensions (3-D).[7]

Because rectus EOMs travel through their respective pulleys, they must lie along the EOM paths, which are not transversely inflected in central gaze. This allows rectus pulley coordinates in 2-D to be reasonably estimated for central gaze from the most anterior EOM cross sections observed in MRIs taken in quasicoronal planes (perpendicular to the long axis of the orbit). This approach, which does not require extremely fine imaging resolution, has demonstrated consistent EOM pulley positions in the quasicoronal plane in normal subjects.[5,7] In secondary gaze positions, higher resolution MRI in normal subjects demonstrates sharp inflections in rectus EOM paths occurring at the pulleys.[7] Posterior to the pulleys, EOM paths are largely independent of gaze position, whereas anteriorly the paths are directly observed to follow transversely inflected straight paths toward their moving insertions on the sclera. Both large and small abnormalities of pulley locations in the coronal plane have been associated with incomitant strabismus that can mimic oblique EOM dysfunction.[8–10]

Beyond static malpositioning of pulleys, it seems plausible that pulley instability causing sideslip of rectus EOMs during ocular rotations may cause incomitant strabismus. Dynamic changes in pulley position occur physiologically during gaze shifts. These changes include large pulley shifts along the EOM's longitudinal axis, because the orbital layer (OL) inserts on the pulley and translates it posteriorly during contraction,[6] and because of small but systematic transverse changes in the coronal plane due to mechanical intercouplings among pulleys[5] and the actions of the of oblique EOM OLs.[11,12] However, strabismus associated with severe dynamic transverse instability of EOM pulleys has not been studied systematically. Precise anatomic determination of pulley position as a function of gaze is necessary to understand this mechanism as a potential cause of incomitant strabismus. In the present study, we used high-resolution MRI to characterize instabilities of rectus EOM pulleys during gaze shifts in patients who had incomitant strabismus, in which the angle of deviation depends on gaze direction.

Methods

We studied six volunteers who had incomitant strabismus. All subjects underwent complete ophthalmic examinations and photography in diagnostic gaze positions. One volunteer without strabismus contrib-

From the Jules Stein Eye Institute, Departments of [1]Ophthalmology and [4]Neurology, University of California, Los Angeles, California; [2]Department of Ophthalmology, Samsung Medical Center, Sungkyunkwan University School of Medicine, Seoul, Korea; and the [3]Southern California Permanente Medical Group, Woodland Hills, California.

Supported by Grant EY08313 and Core Grant EY00331 from the National Eye Institute. JLD received a Research to Prevent Blindness Lew R. Wasserman merit award and is Laraine and David Gerber Professor of Ophthalmology.

Submitted for publication February 28, 2001; revised January 29, 2002; accepted February 6, 2002.

Commercial relationships policy: N.

The publication costs of this article were defrayed in part by page charge payment. This article must therefore be marked "*advertisement*" in accordance with 18 U.S.C. §1734 solely to indicate this fact.

Corresponding author: Joseph L. Demer, Jules Stein Eye Institute, 100 Stein Plaza, UCLA, Los Angeles, CA 90095-7002; jld@ucla.edu.

uted control data that were analyzed to assure consistency with data previously published.[7] After obtaining written informed consent according to a protocol conforming to the Declaration of Helsinki and approved by the Institutional Review Board at the University of California, Los Angeles, subjects underwent high-resolution, T_1-weighted MRI with a 1.5-T scanner (Signa; General Electric, Milwaukee, WI). Each subject's head was carefully stabilized supine with the nose aligned to the longitudinal and the pupils to the transverse light projection references of the scanner. An array of four surface coils was deployed in phased pairs, two over each orbit, in a masklike enclosure held strapped to the face. An adjustable array of monocular, afocal, illuminated fixation targets at nine diagnostic positions of gaze was secured 2.5 cm in front of each orbit with the center target in subjective central position for each eye. Eccentric targets were placed at the maximum eccentricities that could be maintained by subjects for the duration of scanning, and usually at least 20° from central gaze. Targets were visible to one eye only, whereas the other eye was in darkness inside the scanner bore. Subjects were repeatedly coached to avoid unnecessary movements during scanning. Blinking was reduced by maximizing precorneal humidity with a transparent facemask and instructing subjects to avoid unnecessary blinks. Head movement was minimized by secure stabilization to the surface coil facemask and judicious use of padded restraints.

Axial images were obtained at 3.0-mm thickness using a 256×192 matrix over a 10-cm^2 field to localize placement of subsequent higher resolution quasicoronal images perpendicular to the orbital axis. These axial images were obtained only to facilitate subsequent imaging, because axial or sagittal images are not appropriate for quantitative analysis of rectus EOM paths.[13] Multiple contiguous quasicoronal MRIs 2-mm thick (3 mm in the case of subject 6) were then obtained using a 256×256 matrix over an 8-cm^2 field, giving pixel resolutions of 313 μm. Imaging was repeated in central gaze, infraduction, supraduction, abduction, and adduction, with a scan duration of 3.5 minutes. Digital MRIs were transferred to computers (Macintosh; Apple Computer, Cupertino, CA), converted into 8-bit tagged image file format (TIFF) using locally developed software, and quantified using NIH Image (W. Rasband, National Institutes of Health; available by ftp from zippy.nimh.nih.gov or on floppy disc from NTIS, Springfield, VA, part number PB95-500195GEI).

Each rectus EOM location was determined by its area centroid, equivalent to the center of gravity of a shape of uniform density and thickness.[7] Quantitative analysis of MRIs requires the following consideration of individual subject variation in orbital size, and angular and linear head orientation in the scanner. Initially, data for each of the rectus EOMs was collected in Cartesian scanner coordinates from the original MRIs. Data were transformed by a sequence of rotations into a standard coordinate system as previously described,[7] and only a brief summary follows. Approximating the globe as spherical, its 3-D center was determined to subpixel resolution in scanner coordinates, using curve-fitting to three cross-sectional images of the globe, as previously described.[5,14] This operation permits determination of the globe center at subpixel resolution, because the center is not determined from any one pixel, but from combined data representing all the pixels in three complete globe cross sections. This method is not significantly compromised by asphericity of the globe in pathologic cases. Analytical simulations with globes distorted from sphericity by up to 25% result in a maximal error in globe center determination of only approximately 0.15 mm. All rectus EOM positions were then translated to place the 3-D coordinate origin at the computed center of the globe. After translation, the data were rotated about the globe center using extraorbital landmarks (no suitable global referents exist).[7] First, a horizontal rotation (yaw) was performed to align the interhemispheric fissure of the brain, which direction was taken as true anteroposterior. A vertical rotation (pitch) was then performed to bring the junction of the superior ethmoid air sinus and the orbit to the standard angle of 10° elevation from true horizontal. An illustration of this consistent landmark has been published.[7] This vertical rotation was selected to be 10°, because it was the mean angle required to bring the MR to true horizontal in the first 20 orbits analyzed. Finally, a torsional rotation (roll) was performed to bring the interhemispheric fissure of the brain to true vertical. The skull and globe were assumed to be rigid bodies. Consequently, points on either could be shifted by both rotation and translation relative to the coordinate system. The geometric center of the globe was used as the origin of the transformed coordinate system in which EOM area centroids were represented, but this analysis makes no assumptions about actual center of rotation of the eye. After transformation, scanner coordinates were scaled to millimeters, and were further scaled to normalize each globe to the measured average diameter of 24.3 mm.[7] Displacement of the globe–optic nerve junction from its position in central gaze was used to estimate ocular rotation, as previously described.[7] In interpreting such data, it is helpful to recognize that earlier studies have shown rectus EOM paths near the orbital apex to be highly stable over the range of gaze,[7] consistent with histologic evidence of the rigid EOM origins and other connective tissue constraints in that region.[15] Therefore, apparent parallel shifts in EOM paths near the orbital apex must represent globe translation, and any apparent changes in the angles of posterior EOM paths must represent residual angular deviations of the head.

An alternative method of computing globe translation was considered, based on determination of the centroids of the globe and orbit cross sections. This method was rejected as unreliable because of the irregular shape of the orbit. Although slight changes in the image plane have little effect on the location of the centroid of the circular cross section of the globe, they have large and variable effects on the irregular cross section of the orbit. The orbital cross section varies in shape along its anteroposterior axis and varies considerably among subjects.

Computational simulations of binocular alignment were performed, using the Orbit 1.8 computational model of orbital statics,[16] modified to include the normal 3-D locations of the rectus pulleys as determined by MRI in secondary gaze positions.[7] This general modeling approach has been used previously.[10,15] Specific rectus pulley locations for each eye of each subject in central gaze formed the starting point of each simulation. Although this analysis did not account for pulley instability or globe translation, it did suggest the qualitative pattern of incomitance expected from the observed pulley heterotopy in central gaze. Simulations were repeated for informative gaze directions, by using pulley positions measured for those directions. Globe translation was not specifically considered, because nonhomogeneous globe stiffness is not implemented in the Orbit 1.8 model.

Results

Twelve orbits of six subjects with incomitant strabismus were analyzed. Clinical information on the subjects is summarized in Table 1.

General Imaging Features

Area centroids were determined by outlining EOM cross sections (Fig. 1) from near the orbital apex, usually as far anteriorly as the globe equator for the superior rectus (SR), lateral rectus (LR), and inferior rectus (IR). Area centroids of the MR occasionally were outlined anterior to the equator. Figure 1A illustrates, by images obtained in the vicinity of the pulleys, the typical stability of the MR and LR with large vertical gaze shifts. As previously described,[5] the LR pulley shifted inferiorly in the orbit in supraduction, and inferiorly in infraduction, but these small shifts were inconspicuous on casual examination of MRIs in normal subjects. All the subjects with strabismus showed much larger gaze-related shifts in EOM paths, as described later.

The globe itself normally translates with gaze shifts, producing apparent displacement of the orbital area centroid in the oculocentric coordinate system.[5] Because EOMs are firmly an-

TABLE 1. Clinical Characteristics

Subject	Age (y/sex)	Central Deviation	Version Abnormalities		Clinical Diagnosis
			Right Eye	Left Eye	
1	60/F	3 ET 4 LHT 5° Excyclo	Overelevation and underdepression in adduction	Underelevation in abduction and adduction	Axial myopia; AXL: 29.5 mm right, 27.1 mm left
2	38/F	18 E(T) 4 RHT 5–7° Excyclo	Overelevation and underdepression in adduction	Underelevation in abduction	Axial myopia; AXL: 29.4 mm right, 29.3 mm left; V pattern ET
3	33/M	10 X′ 0–3° excyclo	Overdepression in adduction	Overdepression in adduction	X pattern XT; previous XT surgery
4	69/M	6 RHT 7° Eycyclo	—	Marked underelevation in adduction; moderate underelevation in direct supraduction	Simulated Brown syndrome; V pattern XT
5	34/F	Orthotropia 0° Excyclo	—	Overelevation in adduction	V pattern XT
6	10/M	12 XT 0°Excyclo	Underelevation and underdepression in adduction	Underelevation and underdepression in adduction	Marfan syndrome; V pattern XT

AXL, axial length; ET, esotropia; E(T), intermittent esotropia; LHT, left hypertropia; RHT, right hypertropia; excyclo - excyclotropia; X, exophoria; X(T), intermittent exotropia; X′, exophoria at near; XT, exotropia; XT′, exotropia at near.

chored to bone in the orbital apex, globe translation also produces an apparent parallel shift in the posterior EOM path in an oculocentric depiction. Posterior EOM paths are immobilized to the orbital walls by dense connective tissues, and thus cannot actually move. The amount of vertical translation of posterior EOM paths required to superimpose them at the apex was taken to represent the arithmetic negative of globe translation. This method was found to be more accurate than inferring globe translation by comparing globe center with the orbital area centroid, computation of the latter being compromised by marked variations in orbital shape near the globe equator. Data for each rectus EOM were graphically presented in oculocentric depiction, permitting direct comparison of posterior EOM stability with a previous study.[5] Data on 3-D pulley locations are summarized in Table 2, and may be compared with the 95% confidence areas for the normal MR and LR pulleys reported previously.[7] The anteroposterior coordinates of the pulleys were resolvable only to the 2-mm thickness of an image plane and so are reported with confidence limits of ±2 mm.

Axial High Myopia

In both subjects with axial high myopia, one LR pulley was vertically unstable, shifting inferiorly in supraduction, by amounts exceeding that of a group of normal subjects illustrated in Figure 5 of Clark et al.[7]

Subject 1. This 60-year-old woman had V-pattern esotropia and myopia with abnormally great axial length of 29.5 mm in the right eye and 27.1 mm in the left eye. There was moderate overelevation and moderate underdepression in adduction of right eye, and moderate limitation to elevation in both abduction and adduction of left eye. She had 3 prism diopters of esotropia with 4 prism diopters of left hypertropia in central gaze.

The paths and stability of all EOMs in the right orbit were comparable to normal. Figure 2A depicts vertical position of the right MR position in central gaze, elevation, and depression. The MR path in central gaze was approximately a straight line from orbital apex to insertion, continuing through the 95% confidence region of the normal MR pulley (gray rectangle).[7] Anteriorly there was a large inflection of the MR path toward the direction of gaze beginning 4 to 6 mm posterior to globe center. This inflection in MR path indicated the functional pulley location, 13.8 mm medial and 0.3 mm inferior to globe center (Table 2). This is not statistically different from the normal MR pulley position, specified by a confidence interval of 3 ± 2 mm posterior, 14.2 ± 0.2 mm medial, and 0.3 ± 0.3 mm inferior to globe center.[7] The right globe translated 0.3 mm inferiorly in supraduction, similar to reported normal values,[7] but the 1.4-mm superior globe translation in infraduction was greater than the normal 0.5-mm translation.

Figure 2B depicts the vertical position of the right LR in central gaze, supraduction, and infraduction. Again, the LR path was straight from orbital apex to insertion in central gaze. In supraduction, the apparent posterior path of the LR shifted superiorly, reflecting an inferior globe translation of 1.3 mm. In infraduction, the apparent posterior path of the LR shifted inferiorly, reflected in the superior globe translation of 0.3 mm. In both supraduction and infraduction, there was a discrete inflection in the anterior LR path toward the displaced insertion, occurring approximately 9 mm posterior and 10.7 mm lateral to globe center (Table 2). Based on the EOM's course in central gaze, the LR pulley position was significantly inferior to the normal LR pulley position specified by a confidence interval 9 ± 2 mm posterior, 10.1 ± 0.1 mm lateral, and 0.3 ± 0.2 mm inferior to globe center.[7] The inflection point, signifying the LR pulley, shifted 1.3 mm superiorly from infraduction to supraduction, due to inferior globe translation in supraduction and superior globe translation in infraduction. This movement is comparable to the normal LR pulley shift of 1.5 mm.[5]

The left LR pulley was unstable, shifting inferiorly in supraduction (Fig. 1B). The other rectus EOMs on the left had normal paths and pulley positions. Figure 3 shows the vertical position of the left LR in central gaze, supraduction, and infraduction. It was not possible to resolve the LR centroids far enough anteriorly to discern discrete path inflections associated with vertical ductions and so to determine anteroposterior pulley position. Table 2 states lateral and superior coordinates for the LR pulley in central gaze, making the customary assumption that the most anterior identifiable LR centroid was directly in line with its pulley. While in a normal position 9.9 mm lateral to globe center, the left LR pulley had inferior heterotopy, 1.5 mm inferior, based on the LR path in central gaze (Table 2). The normal confidence interval for the vertical

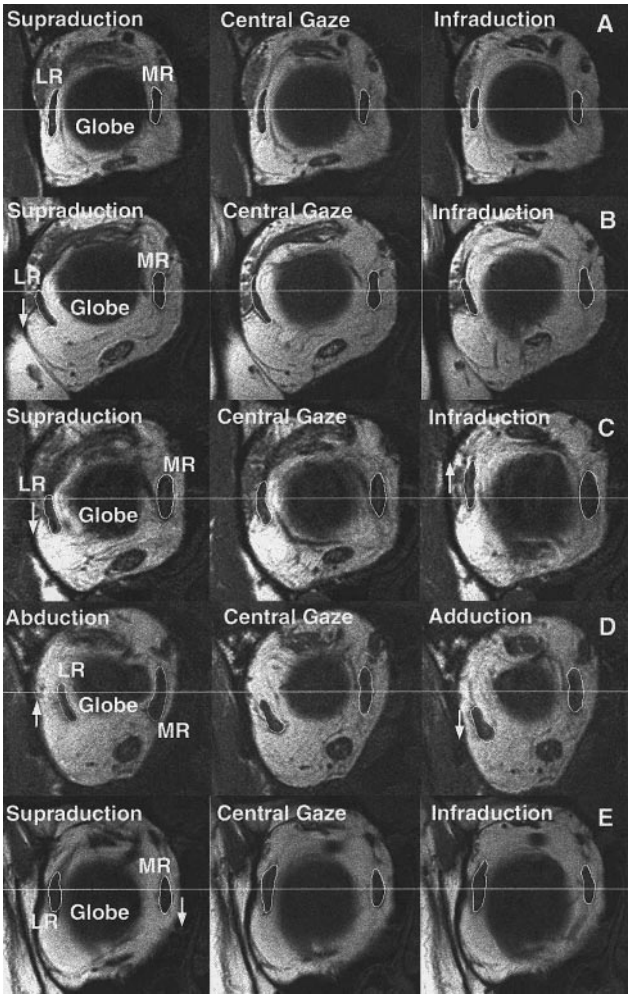

FIGURE 1. Magnetic resonance images of orbits in quasicoronal planes near the pulleys in central gaze and secondary gaze positions. Bellies of the MR and LR are outlined in *white*. Area centroids represent geometric centers of the outlined areas and were used to determine EOM position. Left orbits were rotated horizontally to the configuration of right orbits for analysis. *Thin horizontal white lines*: position references for appreciation of vertical shifts of EOMs. Approximate distances from globe center are provided, representing the range illustrated for the specific EOM for each subject illustrated in subsequent figures, although exact distances were computed for each gaze position. (**A**) Normal subject: In an image plane approximately 8 to 9 mm posterior to globe center, the right MR and LR did not shift during gaze changes. Because image planes are oblique to the coordinate system, the image plane location represents the average location for each of the four rectus EOMs. (**B**) Subject 1: In an image plane approximately 10 to 11 mm posterior to globe center, the left LR shifted inferiorly in supraduction. This image plane corresponds approximately to the *upward arrow* in the plot of the LR path in Figure 3. (**C**) Subject 3: In an image plane approximately 11 to 13 mm posterior to globe center, the right LR shifted inferiorly in supraduction and superiorly in infraduction. This image plane corresponds approximately to the *upward arrow* in the plot of the LR path in Figure 4. (**D**) Subject 4: In an image plane approximately 11 to 14 mm posterior to globe center, the left LR shifted inferiorly in adduction and superiorly in abduction. This image plane corresponds approximately to the *upward arrow* in the plot of the LR path in Figure 5. (**E**) Subject 6: In an image plane approximately 5 to 6 mm posterior to the globe center, the right MR shifted inferiorly in supraduction. This image plane corresponds approximately to the *upward arrow* in the plot of the MR path in Figure 6.

position of the LR pulley is 0.3 ± 0.2 mm inferior to globe center.[7] Although the LR followed a straight path from orbital apex to scleral insertion in central gaze and infraduction, it followed an inferiorly sloping path in supraduction, associated with an increasing inferior displacement of the LR pulley. However, the absence of a parallel shift in the posterior path of the left LR suggested little globe translation. The LR pulley shifted approximately 1 mm inferiorly during the gaze shift from infraduction to supraduction.

Subject 2. This 38-year-old woman had V-pattern esotropia and myopia with axial length 29.4 mm in the right eye and 29.3 mm in the left eye. There was overelevation and underdepression in adduction in the right eye, and underelevation in abduction in the left eye. She had 18 prism diopters of esotropia with 4 prism diopters of right hypertropia in central gaze.

Although EOM pulley location and stability were normal for the right orbit, the left LR pulley was abnormally unstable. All other EOMs in the left orbit had normal path stability with gaze shifts. While in a normal position 9 mm posterior and 10 mm lateral to globe center, the left LR pulley showed marked inferior heterotopy, 1.8 mm inferior (normal confidence interval, 0.3 ± 0.2 mm[7]; Table 2). As judged by the path inflection, the left LR pulley was 9 mm posterior to globe center and shifted by 0.5 mm inferiorly from infraduction to supraduction. The left globe translated a normal amount of 0.2 mm superiorly in infraduction, but a greater than normal amount of 2.1 mm inferiorly in supraduction.[7]

Divergence in Vertical Gaze

Subject 3. This 33-year-old man had undergone strabismus surgery twice in childhood for intermittent exotropia, but had residual X-pattern exotropia measuring 10 prism diopters in central gaze and increasing in both infra- and supraduction. There was overdepression in adduction of both eyes. There was abnormal instability of both LR muscle paths: both LR pulleys shifted inferiorly in supraduction and superiorly in infraduction, as shown for the representative right orbit in Figure 1C. Because of postsurgical changes, it was not possible to reliably follow LR cross sections far enough anteriorly to demonstrate discrete inflections in LR path with vertical gaze shifts, but data from the more posterior LR path were sufficient to demonstrate pulley instability. Figure 4 shows the vertical position of the right LR in central gaze, supraduction, and infraduction. As determined by LR path, the LR pulley was in a normal position in central gaze. The LR pulley shifted by at least 2 mm inferiorly from infraduction to supraduction, an amount roughly double the normal value.[7] The actual shift was probably even greater than this estimate of 2 mm, because inflections in LR path could not be demonstrated, probably because of postsurgical changes. Table 2 states lateral and superior coordinates for the LR pulley in central gaze, making the customary assumption that the most anterior identifiable LR centroid was directly in line with its pulley. As assessed by the most posterior LR path, globe translation did not appear significant.

The left LR behaved similarly to the right. Based on the same assumption as used for the right, the left LR pulley was located 9.8 mm lateral and 0.1 mm inferior to globe center (Table 2) and shifted inferiorly by approximately 1 mm from infraduction to supraduction.

Restrictive Hypotropia in Adduction

Subject 4. This 69-year-old man had idiopathic acquired restrictive limitation to elevation of the left eye in adduction (simulated Brown syndrome), and V-pattern exotropia measuring 10 prism diopters in central gaze. There was marked underelevation in adduction and moderate underelevation in direct supraduction for the left eye. Unlike any of the other subjects, both LR EOMs of subject 4 were displaced inferiorly by approximately 4 mm even near the orbital apex. As the right

TABLE 2. Horizontal Rectus Pulley Positions

Subject		Medial Rectus			Lateral Rectus		
		Anterior	Lateral	Superior	Anterior	Lateral	Superior
Normal		**−3 ± 2**	**−14.2 ± 0.2**	**−0.3 ± 0.3**	**−9 ± 2**	**10.1 ± 0.1**	**−0.3 ± 0.2**
1	Right	−4 to −5.5	−13.8	−0.3	−9	10.7	**−3.2**
	Left	−5	−14.1	−0.3	N/A	9.9	**−1.5**
2	Right	−5	−14.0	−0.5	−9	10.1	−0.5
	Left	−4	−14.5	−0.6	−9	10.0	**−1.8**
3	Right	−6	−13.9	0.1	N/A	10.3	−0.4
	Left	−4	−14.5	−0.3	N/A	9.8	−0.1
4	Right	−6	−13.9	−0.5	−9	9.8	−0.4
	Left	−5	−13.8	0.1	−10	9.8	**−3.8**
5	Right	−4	−14.2	0.1	−9	9.9	−0.5
	Left	−6	−13.8	0.1	−9	9.7	**−1.6**
6	Right	−2	−14.6	**2.0**	−12	10.6	−0.1
	Left	**−9**	−14.7	**0.4**	−12	10.3	0.1

Data are expressed in millimeters, relative to globe center. Values in bold are significantly abnormal. Anterior positions were determined from EOM path inflections in secondary gaze positions, where available. Lateral and superior positions were determined from EOM paths in central gaze, and do not account for translations in eccentric gazes. N/A, anteroposterior position not available due to inability to resolve the EOM path inflection in secondary gaze positions.

LR traveled anteriorly, it also moved superiorly to a normally located pulley, having normal stability with gaze shifts. This was not the case for the left LR (Fig. 1D). While in a normal position 10 mm posterior and 9.8 mm lateral to globe center, the left LR pulley had marked inferior heterotopy, 3.8 mm inferior (normal confidence interval, 0.3 ± 0.2 mm[7]; Table 2). Based on the plausible and qualitatively supported assumption that even though the LR origin in the orbital apex was inferior to normal, the LR was nevertheless fixed at its origin in the orbital apex, the globe translated inferiorly by approximately 3 mm in abduction and infraduction. The globe translated 1.5 mm inferiorly in adduction, where there was an inferior inflection in LR path 13 mm posterior to globe center, posterior to the normal location of the LR pulley[7] (Figs. 1D, 5). The LR was thus more inferior in adduction than in infraduction (Fig. 5). Pulley locations and stability were normal in the other EOMs.

The right globe translated 0.2 mm superiorly in infraduction, 0.1 mm inferiorly in abduction, and 0.1 mm inferiorly in adduction. These values are within the normal range.[7] The left globe translated 0.5 mm superiorly in infraduction, 0.6 mm superiorly in abduction, and 0.5 mm inferiorly in adduction, the latter two values exceeding normal.[7]

During strabismus surgery, the left globe could not be elevated passively in adduction, although this was possible in abduction. The restriction to elevation in adduction was not relieved by nasal tenotomy of the left SO. The LR was observed to run in an abnormal inferior course from its insertion, a malposition exaggerated in adduction and consistent with the MRI. After the superior border of the LR was sutured to the underlying sclera approximately 8 mm posterior to the insertion, some of the restriction to elevation of the left globe in adduction was relieved, even after reanastomosis of the SO tendon. The clinical limitation to elevation in adduction was improved after surgery, and the left hypotropia in central gaze was corrected.

V-Pattern Exotropia

Subject 5. This 34-year-old woman had V-pattern exotropia that diminished in depression, and overelevation in adduction of the left eye. The left LR pulley was heterotopic. While in a normal position 9 mm posterior and 9.7 mm lateral to globe center, the left LR pulley had marked inferior heterotopy, 1.6 mm inferior (Table 2). Instability of the left LR path was revealed by MRI. The left LR pulley shifted by 0.7 mm inferiorly with shift from central gaze to adduction. Anteriorly, there was a large inferior deflection of the LR path in both infraduction and adduction. The globe translated 0.2 mm inferiorly in supraduction, 0.1 mm superiorly in abduction, 0.6 mm superiorly in infraduction, and 0.8 mm superiorly in adduction. These values are comparable to normal, except adduction, in which they exceeded normal.[7]

Subject 6. This 10-year-old boy had Marfan syndrome (MFS), based on multiple cardiovascular and skeletal abnormalities, as well as bilateral lens subluxation. There was V-pattern exotropia measuring 12 prism diopters in central gaze, and increasing with supraduction. There was underelevation and underdepression in adduction of both eyes. While in a normal position 14.6 mm medial to globe center, the right MR pulley showed heterotopy, being 2 mm posterior and 2 mm superior (Table 2). The normal confidence interval for the MR pulley is 3 ± 2 mm posterior and 0.3 ± 0.3 mm inferior to globe center.[7] MRI revealed abnormal instability of both MRs, which shifted inferiorly in supraduction (Fig. 1E). Figure 6 shows the vertical position of the right MR in central gaze, supraduction, and infraduction. Based on the discrete inflection in infraduction, the MR pulley was located approximately 2 mm posterior to globe center, an anteroposterior position within the 95% normal confidence limit.[7] In supraduction, the MR followed an arc inferiorly beginning around 9 mm posterior to globe center, presumably the region of the MR pulley sleeve. It was not possible to resolve the MR centroid sufficiently far anteriorly to demonstrate a discrete inflection in MR path in supraduction, but from the available MR path data the MR pulley must have shifted inferiorly by approximately 2 mm from infraduction to supraduction. Based on the posterior MR path, the globe translated 0.4 mm inferiorly in supraduction, and 1.5 mm inferiorly in infraduction.

Behavior of the left MR and globe were similar to that of the right. While in a normal position 14.7 mm medial to globe center, the left MR pulley had posterior and superior heterotopy, being 9 mm posterior and 0.4 mm superior (Table 2). The left MR pulley shifted by 0.6 mm inferiorly from infraduction to supraduction. The left globe translated 1.2 mm superiorly in

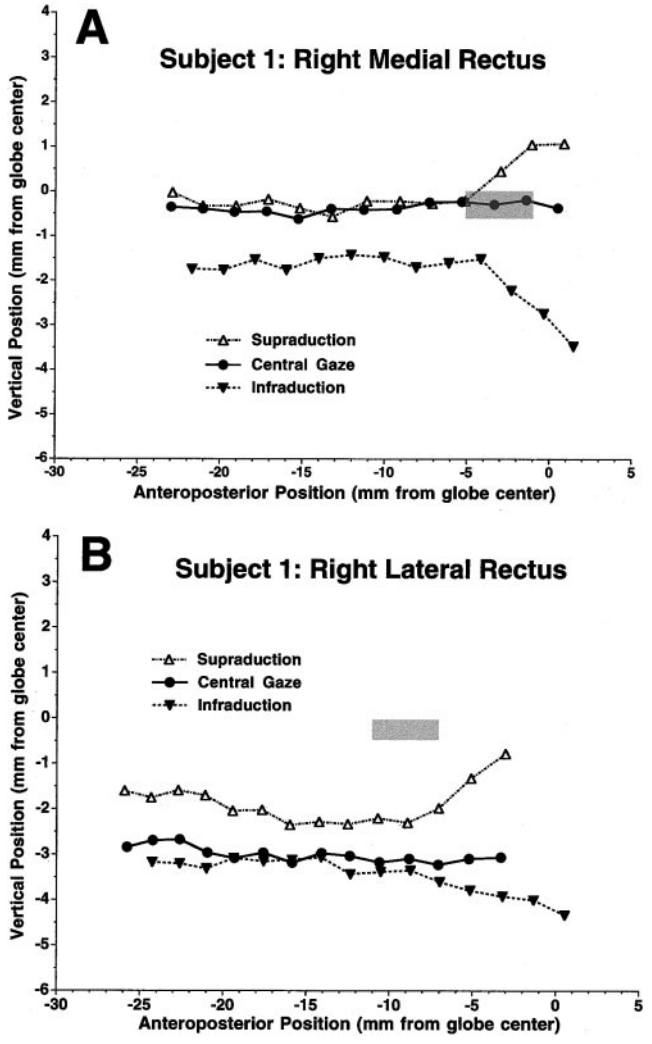

FIGURE 2. Subject 1: (**A**) vertical area centroid positions of the right MR along the anteroposterior orbital axis, referenced to globe center. The posterior path showed little sideslip, but in supraduction there was a parallel shift attributable to superior globe translation. The anterior MR path showed discrete inflection superiorly in supraduction, and inferiorly in infraduction, beginning approximately 5 mm posterior to globe center, and within the 95% confidence region for the normal MR pulley (*gray rectangle*).[7] (**B**) Vertical area centroid positions of the right LR along the anteroposterior orbital axis, relative to globe center. The posterior path exhibited a superior parallel displacement in supraduction. There was discrete inflection superiorly in supraduction and inferiorly in infraduction, beginning approximately 9 mm posterior to globe center, well inferior to the 95% confidence region for the normal LR pulley (*gray rectangle*).[7]

infraduction and 0.5 mm inferiorly in supraduction, appreciably more than normal.[7]

Computational Simulations

Computational simulations of binocular alignment were performed using the Orbit 1.8. model. Pulley locations measured in central gaze positions alone qualitatively predicted the V patterns in subjects 1, 2, 4, 5, and 6 and the X pattern in subject 3. This suggests that the static pulley heterotopies might have been partial causes of the incomitancies observed. However, the patterns over a ±30° range of vertical gaze were small—at most, a few degrees. Simulations in selected gaze positions suggested that pulley shifts and globe translation might substantially exaggerate the incomitancies. This interpretation is

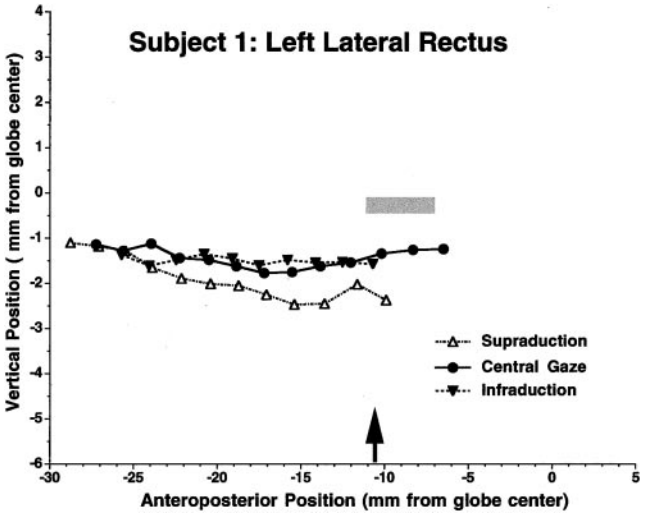

FIGURE 3. Subject 1: vertical area centroid positions of the left LR along the anteroposterior orbital axis, referenced to globe center. The LR path was consistent with a 1.5 mm inferior displacement of its pulley, even in central gaze, well inferior to the 95% confidence region for the normal LR pulley (*gray rectangle*).[7] The posterior LR path displaced farther inferiorly in supraduction, consistent with inferior displacement of the pulley. The LR could not be resolved sufficiently far anteriorly to demonstrate path inflections in supraduction and infraduction. *Upward arrow*: approximate location of image plane depicted in Figure 1B.

necessarily qualitative, due to limitations on the Orbit 1.8 simulations discussed below.

DISCUSSION

Pulleys in Ocular Motility

Rectus EOMs are encircled by their pulleys, so pulleys must lie along the EOM paths. Because the pulleys cannot be directly

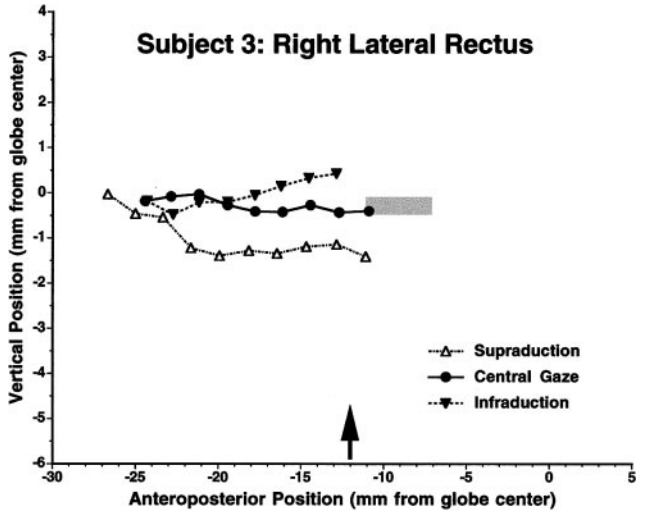

FIGURE 4. Subject 3: vertical area centroid positions of the right LR along the anteroposterior orbital axis, referenced to globe center. The LR path in central gaze was consistent with the 95% confidence region for the normal LR pulley (*gray rectangle*).[7] The posterior path displaced superiorly in infraduction and inferiorly in supraduction, consistent with pulley instability. The LR could not be resolved sufficiently far anteriorly to demonstrate path inflections in supraduction and infraduction. *Upward arrow*: approximate location of image plane depicted in Figure 1C.

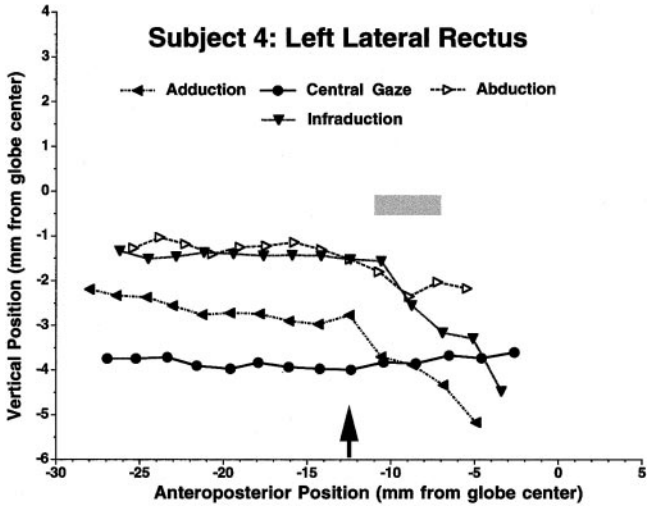

FIGURE 5. Subject 4: vertical area centroid positions of the LR along the anteroposterior orbital axis, referenced to globe center. The LR path in central gaze was consistent with a marked inferior displacement of the LR pulley, well inferior to the 95% confidence region for the normal LR pulley (*gray rectangle*).[7] The parallel shifts in the LR path in secondary gaze positions were consistent with globe translation. In both depression and adduction, there was a discrete inferior inflection in LR path, located posterior to the normal pulley location in the latter case. *Upward arrow*: approximate location of image plane depicted in Figure 1D.

imaged in most cases, their locations must be inferred from the paths of EOMs, which can be imaged by MRI. In central gaze, the coronal plane locations of rectus pulleys can be inferred from the rectus EOM paths, which bow slightly away from the orbital center,[17] but in this gaze direction are not otherwise inflected. This approach has demonstrated normal rectus pulleys to be stereotypically placed at precise locations in the coronal plane[5,7] and, normally, to move little with gaze shifts within this plane.[5] Demonstration of the anteroposterior location of rectus pulleys requires identification of discrete inflections in EOM paths toward secondary[7] and tertiary[18] gaze positions. Such discrete, transverse inflections are best demonstrated by imaging in thin, quasicoronal image planes perpendicular to the orbital axis, although this limits anteroposterior resolution of pulley location to roughly the image plane thickness of 2 mm. (The discrete, transverse inflections produced by pulleys in secondary and tertiary gaze positions probably correlate roughly with outward bowing in relaxed rectus EOM paths, due to distributed pulley suspensory tissues, but this outward bowing behavior does not define the more focal pulley inflections that are kinematically significant.) In contrast to the transverse stability and resistance to EOM sideslip, coronal plane MRI in tertiary gaze positions shows normal rectus pulleys to be highly mobile along the axes of their respective EOMs,[18] probably because of the insertions of the EOM orbital fiber layers on the pulleys.[6] The anteroposterior position of each rectus pulley appears to be actively controlled consistent with the 3-D kinematics of Listing's law during visually guided eye movements[6,18] and may be differently controlled during the vestibulo-ocular reflex[6,15] and convergence.[19] Autonomically innervated smooth muscle is also distributed in pulley suspensions in a manner that could provide fine adjustments in the coronal plane locations of rectus pulleys,[3] but direct evidence of this behavior is currently unavailable. Precise 3-D position of pulleys implements a linear oculomotor plant that appears commutative in the mathematical sense to neural control mechanisms in the brain,[20,21] making control of eye orientation independent of the sequential history of eye movements.

In view of the importance of precise pulley location to ocular motor control, it is not surprising that the stable malpositioning of pulleys—-heterotopy—-is strongly associated with strabismus. Biomechanical modeling consistently predicts the individual patterns of incomitant strabismus observed in patients in whom orbital MRI has determined abnormal pulley locations.[9,10] The absence of significant pulley heterotopy in cases of SO palsy with significant excyclotropia argues that the coronal plane pulley heterotopy observed in other cases is the cause, rather than the result, of strabismus.[22] Pulley heterotopy is associated with facial dysmorphism, presumably because both are due to malformation of the bony orbit.[23] Surgical interference with the normal anteroposterior travel of rectus pulleys produces a restriction to ocular rotation in the field of action of the involved EOM.[24] Large, presumably acquired lateral rectus pulley heterotopy in axial high myopia produces an extreme, fixed esotropia and hypotropia.[25–28]

Unstable Pulleys in Current Subjects

The current report extends the spectrum of pulley abnormalities to include dynamic instability. Six subjects were identified with incomitant strabismus featuring V- or X-pattern incomitance, or restrictive hypotropia in adduction. All subjects had a factor predisposing to acquired weakness of rectus pulley suspensions: degeneration associated with axial high myopia[25–28] or the elastic tissue defect in MFS,[29] repeated prior surgery of rectus EOMs,[15] or advanced age. Apparently, normal aging is associated with acquired limitation of supraduction[30] and with pulley shifts suggestive of connective tissue laxity.[30] All the current subjects with incomitant strabismus except subject 3 had at least one rectus pulley location that was significantly outside the 95% confidence limits of normal,[5,7]

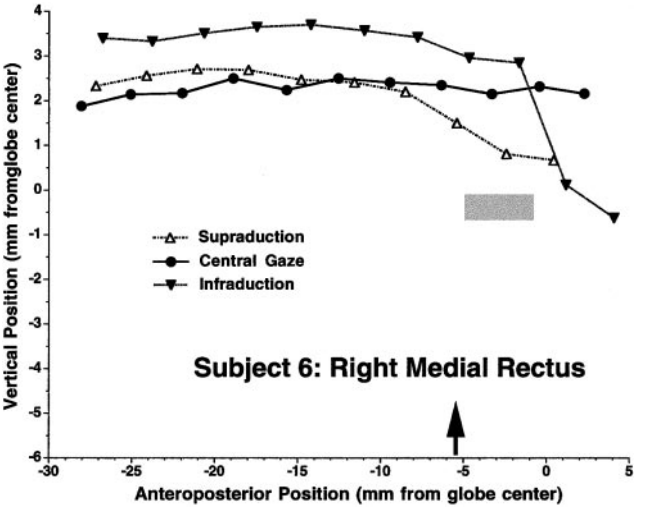

FIGURE 6. Subject 6: vertical area centroid positions of the MR along the anteroposterior orbital axis, referenced to globe center. The MR path in central gaze was consistent with a marked superior displacement of the MR pulley, significantly superior to the 95% confidence region for the normal MR pulley (*gray rectangle*).[7] The anterior EOM path showed discrete inflection inferiorly in infraduction beginning approximately 2 mm posterior to globe center and associated with a 1.5 mm inferior globe translation that appears to offset the posterior path of the MR superiorly. In supraduction, the MR path just posterior to the pulley region made a gradual curve inferiorly, but the MR could not be followed far enough anteriorly to demonstrate the pulley inflection. *Upward arrow*: approximate location of image plane depicted in Figure 1E.

and all subjects had at least one pulley that shifted substantially more than normal with gaze shifts to secondary gaze positions. Pulley heterotopy was thus common in these subjects.

The coordinated control postulate of the active pulley hypothesis proposes that normal rectus pulleys shift anteroposteriorly along the axes of their respective EOMs during gaze shifts and predicted that this corresponds to the amount of anteroposterior shift in EOM path inflections in tertiary gaze positions.[6,18] Although MRI in tertiary gaze positions confirms this prediction in normal subjects,[18] this anteroposterior pulley shift is physiologic and thus distinct from the pathologic transverse pulley instability evident in the present study. Determination of pulley locations by MRI suggests that dynamic instability of pulleys and the globe center may have been causally related to the specific patterns of strabismus in all subjects, with specific patterns of incomitance also related to static pulley heterotopy. Computational simulation using the Orbit 1.8 model of the expected effect of the static pulley heterotopies in all subjects qualitatively matched their observed incomitant patterns of strabismus. Although the globe normally translates slightly with gaze shifts,[7] all the subjects with incomitant strabismus had significantly greater horizontal and vertical globe translation with gaze. The present methods cannot determine anteroposterior globe translation, and this translation could have occurred without detection.

Interpretation of the effects of pulley instability and globe translation necessarily must be more qualitative, because, although the Orbit 1.8 model is the most complete quantitative description of orbital static mechanics, it does not implement several biomechanical features recently recognized to be important. Although Orbit 1.8 represents each rectus pulley as a point passively suspended from the orbit by homogeneous elasticity, recent evidence indicates that each rectus pulley is actively positioned against a spatially nonuniform elastic load by the action of the orbital layer of the EOM inserting on the pulley.[6] Orbit 1.8 incorporates a mildly stiff pulley for the inferior oblique (IO) that is displaced only by IO tension; recent evidence indicates that the IO has a pulley that is partially coupled to the IR pulley, and that the orbital layer of the IO inserts both on the IO and LR pulleys, producing stereotypic gaze-related shifts in the positions of both.[11,12,31,32] Orbit 1.8 models globe translation by force balance against a uniform elastic stiffness; more realistically, the globe is cradled by interconnections among the mobile rectus and oblique pulleys, whose antagonist pairs normally translate in reciprocal fashion.[6] It is insufficient merely to insert pulley positions measured in secondary gaze positions into a model of binocular statics; the model will not generally be predictive unless the mechanical determinants of pulley positions also are implemented correctly, so that pulley position relative to the globe is generally predicted as a function of gaze. Implementation of such a realistic approach to modeling orbital biomechanics will be a complex undertaking.

In addition to this qualitative evidence suggesting that pulley abnormalities may have caused the strabismus, the pulley instabilities with gaze shifts were plausibly related to individual patterns of incomitance. An inferior shift of the LR in supraduction would increase its elastic tension in that gaze position, tending to produce greater abduction and thus the typical V pattern. The large inferior shift of the left LR pulley in adduction in subject 4 would be expected to redirect the passive elastic force of the LR inferiorly, even with reduced active innervation of the LR. This would account for restrictive hypotropia and limited elevation in adduction and also the observed ipsilateral hypotropia in elevation.

Could the observed pulley instabilities in these subjects have been the result, rather than the cause, of their incomitant strabismus? This possibility seems unlikely, because pulley instability in the current subjects was limited to one EOM in each affected orbit. A generalized disturbance of stability of the entire pulley system that hypothetically might have been produced, for example, by ocular torsion, would have been expected to shift the positions of all the rectus pulleys in a predictable manner. There is evidence that ocular torsion does not necessarily alter rectus pulley position. Such a hypothetical systematic change in static pulley position is absent in superior oblique palsy, even though ocular torsion occurs.[22]

In understanding the roles of subtle pulley instabilities and globe translations in the etiology of strabismus, it is important to bear in mind that the pulling direction of an EOM is determined by its path from pulley to scleral insertion. Location of the anatomic EOM origin in the orbital apex is no more relevant to the rectus EOM's pulling direction than is the anatomic origin of the SO muscle, because both pass through pulleys. Because the length of rectus EOMs anterior to their pulleys is only 12 to 14 mm,[7] small changes in the relative position of pulley insertion due to pulley or globe translation can appreciably redirect the EOM's force. Thus, a 1.5 mm globe translation changes the pulling direction of a typical rectus EOM by 6°. The present cases illustrate that much larger translations can readily occur, and probably produce strabismus by this previously unappreciated mechanism. It is likely that the current data are not fully informative about the complex mechanical relationships occurring in individuals such as subject 6, in whom the globe was enlarged and both the globe and pulleys translated with gaze. Higher-resolution orbital imaging may be required to clarify the mechanics, but it is clear that pulley instability plays a role. Pulley instability should be added to the list of abnormalities that may cause strabismus, including pulley heterotopy and disorders of EOM length, stiffness, innervation, and insertional site.

Connective Tissue Disorders and Pulley Instability

Myopic strabismus fixus (MSF) is a syndrome of monocular or binocular high axial myopia, typically more than 25 D, with large angle esotropia, hypotropia, and limitation of abduction.[25–27,33] It has also been called the "heavy eye" syndrome,[33] reflecting the archaic concept that gravity may cause an elongated, myopic eye to deviate downward. Although early theories suggested that the enlarged globe caused LR atrophy by chronic compression of the LR against the orbital wall,[33,34] modern imaging shows that such patients have marked EOM path abnormalities, with the LR displaced inferonasally. This converts the abducting action of the LR to depression.[25,27] Orbital MRI suggests that MSF is associated with thinning and dehiscence of the connective tissue septum connecting the MR and LR pulleys.[13] It seems likely that MSF is due to a local connective tissue disorder involving sclera and choroid (producing axial myopia) and the EOM pulleys (producing strabismus). Likely candidates for abnormality include fibrillin, elastin, smooth muscle cells, and myofibroblasts.[35] We propose that axially myopic subjects 1 and 2 may have a milder, dynamic form of inferior slippage of the LR pulley as the cause of their strabismus.

The clinical picture of restrictive hypotropia in adduction in subject 4 would traditionally be diagnosed as acquired Brown syndrome, although, with the information available from MRI, the diagnosis of simulated Brown syndrome would be more appropriate. Brown syndrome has been regarded to be a disorder of passage of the SO tendon through its pulley, and MRI imaging has demonstrated multiple abnormalities, including tendon cysts in some cases.[36] The frequent failure of SO surgery to alleviate Brown syndrome fully has been puzzling.[37–39] Convincing evidence that LR pulley instability was instead the

cause of the restrictive hypotropia in subject 4 was provided by the surgical observations. Nasal tenotomy of the SO did not relieve the restrictive hypotropia in adduction, whereas surgical stabilization of the unstable LR pulley provided relief even after reanastomosis of the SO tendon. Similar clinical observations in other cases suggest that LR pulley instability may be a common cause of restrictive hypotropia in adduction clinically indistinguishable from Brown syndrome.[40] Orbital imaging in multiple gaze positions may be clinically valuable for diagnosis of this condition.

MFS is an autosomal dominant condition typified by skeletal abnormalities, valvular and aortic disease, joint hypermobility, atrophic skin streaks, lens subluxation, high myopia, and strabismus.[41] It is caused by mutations in the *FBN-1* gene,[41,42] which codes for the glycoprotein fibrillin.[43] Fibrillin forms the core of microfibrils in elastin fibers and the binding among smooth muscle cells,[44] and is abundant in the pulley suspensions.[29] The significantly elevated prevalence of strabismus in MFS, ranging from 19% to 39%[45,46] has motivated speculation that the deviations are due to abnormal connective tissue laxity.[46] This absence of adequate structural support for pulleys plausibly leads to gaze-related pulley shifts or globe translation, as observed in subject 6 with MFS. It has been recently proposed that age-related degeneration of normal microfibrils is similar to the changes of MFS.[47] This suggests that pulley abnormalities in MFS may reflect an exaggeration of the connective tissue changes observed in normal aging, and that some age-related strabismus may be due to connective tissue degeneration.

References

1. Koornneef L. New insights in the human orbital connective tissue: result of a new anatomical approach. *Arch Ophthalmol.* 1977;95: 1269–1273.
2. Demer JL, Miller JM, Poukens V, Vinters HV, Glasgow BJ. Evidence for fibromuscular pulleys of the recti extraocular muscles. *Invest Ophthalmol Vis Sci.* 1995;36:1125–1136.
3. Demer JL, Poukens V, Miller JM, Micevych P. Innervation of extraocular pulley smooth muscle in monkeys and humans. *Invest Ophthalmol Vis Sci.* 1997;38:1774–1785.
4. Miller JM. Functional anatomy of normal human rectus muscles. *Vision Res.* 1989;29:223–240.
5. Clark RA, Miller JM, Demer JL. Location and stability of rectus muscle pulleys inferred from muscle paths. *Invest Ophthalmol Vis Sci.* 1997;38:227–240.
6. Demer JL, Oh SY, Poukens V. Evidence for active control of rectus extraocular muscle pulleys. *Invest Ophthalmol Vis Sci.* 2000;41: 1280–1290.
7. Clark RA, Miller JM, Demer JL. Three-dimensional location of human rectus pulleys by path inflections in secondary gaze positions. *Invest Ophthalmol Vis Sci.* 2000;41:3787–3797.
8. Demer JL, Miller JM, Poukens V. Surgical implications of the rectus extraocular muscle pulleys. *J Pediatr Ophthalmol Strabismus.* 1996;33:208–218.
9. Clark RA, Miller JM, Rosenbaum AL, Demer JL. Heterotopic rectus muscle pulleys or oblique muscle dysfunction? *J Am Assoc Pediatr Ophthalmol Strabismus.* 1998;2:17–25.
10. Demer JL. Heterotopy of extraocular muscle pulleys causes incomitant strabismus. In: Lennerstrand G, ed. *Advances in Strabismology.* The Netherlands: Aeolus Press; 1999:91–94.
11. Demer JL, Oh SY, Poukens V. Orbital layers of the oblique extraocular muscles (EOMs) insert on the orbital connective tissue system [ARVO Abstract]. *Invest Ophthalmol Vis Sci.* 2001;42(4): **S**517.Abstract nr 2781.
12. Demer JL. The orbital pulley system: a revolution in concepts of orbital anatomy. *Ann NY Acad Sci.* 2002;956:17–32.
13. Demer JL, Miller JM. Orbital imaging in strabismus surgery. In: Rosenbaum AL, Santiago P, ed. *Advanced Strabismus Surgery. Principles and Surgical Techniques.* New York: Mosby; 1999: 84–98.
14. Mason TE, Hazard CT. *Brief Analytic Geometry.* Boston: Ginn & Company, 1935:72.
15. Demer JL. Extraocular muscles. In: Jaeger EA, Tasman PR, ed. *Clinical Ophthalmology.* Vol 1. Philadelphia: Lippincott; 2000: chap 1.
16. Miller JM, Pavlovski DS, Shaemeva I. Orbit 1.8 *Gaze Mechanics Simulation.* San Francisco: Eidactics, 1999.
17. Simonsz HJ, Harting F, de Waal BJ, Verbeeten BWJM. Sideways displacement and curved path of recti eye muscles. *Arch Ophthalmol.* 1985;103:124–128.
18. Kono R, Clark RA, Demer JL. Active pulleys: magnetic resonance imaging of rectus muscle paths in tertiary gazes. *Invest Ophthalmol Vis Sci.* 2002;43:2179-2188.
19. Demer JL, Kono R, Wright W. Magnetic resonance imaging (MRI) of human extraocular muscles (EOMs) during asymmetrical convergence [abstract]. 2002 Annual Meeting Abstract and Program Planner accessed at www.arvo.org. Association for Research in Vision and Ophthalmology. Abstract 1460.
20. Quaia C, Optican LM. Commutative saccadic generator is sufficient to control a 3-D ocular plant with pulleys. *J Neurophysiol.* 1998; 79:3197–3215.
21. Porrill J, Warren PA, Dean P. A simple control laws generates Listing's positions in a detailed model of the extraocular muscle system. *Vision Res.* 2000;40:3743–3758.
22. Clark RA, Miller JM, Demer JL. Displacement of the medial rectus pulley in superior oblique palsy. *Invest Ophthalmol Vis Sci.* 1998; 39:207–212.
23. Velez FG, Clarz RA, Demer JL. Facial asymmetry in superior oblique palsy and pulley heterotopy. *J Am Assoc Pediatr Ophthalmol Strabismus.* 2000;4:233–239.
24. Clark RA, Isenberg SJ, Rosenbaum SJ, Demer JL. Posterior fixation sutures: a revised mechanical explanation for the fadenoperation based on rectus extraocular muscle pulleys. *Am J Ophthalmol.* 1999;128:702–714.
25. Krzizok T, Wagner D, Kaufmann H. Elucidation of restrictive motility in high myopia by magnetic resonance imaging. *Arch Ophthalmol.* 1996;115:1019–1027.
26. Krzizok TH, Kaufman H, Traupe H. New approach in strabismus surgery in high myopia. *Br J Ophthalmol.* 1997;81:625–630.
27. Krzizok TH, Schroeder BU. Measurement of recti eye muscle paths by magnetic resonance imaging in highly myopic and normal subjects. *Invest Ophthalmol Vis Sci.* 1999;40:2554–2560.
28. Demer JL, Miller JM. Orbital imaging in strabismus surgery. In: Rosenbaum AL, Santiago AP, eds. *Clinical Strabismus Management: Principles and Techniques.* Philadelphia: WB Saunders; 1999:84–98.
29. Demer JL, Poukens V. Fibrillin (FBN), elastin, and smooth muscle in the extraocular muscle pulleys in Marfan syndrome (MFS) [ARVO Abstract]. *Invest Ophthalmol Vis Sci.* 1998;39(4):**S**1102. Abstract nr 5096.
30. Clark RA, Demer JL. Effect of aging on human rectus extraocular muscle paths demonstrated by magnetic resonance imaging. *Am J Ophthalmol.* In press.
31. Demer JL, Miller JM. Dynamic magnetic resonance imaging of the inferior oblique muscle in normal and strabismic subjects. *Abstracts of the American Association for Pediatric Ophthalmology and Strabismus.* 1997;11.
32. Demer JL, Clark RA, Miller JL. Magnetic resonance imaging (MRI) of the functional anatomy of the inferior oblique (IO) muscle [ARVO Abstract]. *Invest Ophthalmol Vis Sci.* 1999;40(4):**S**772. Abstract nr 4073.
33. Kowal L, Troski M, Gilford E. MRI in the heavy eye phenomenon. *Aust NZ J Ophthalmol.* 1994;22:125–126.
34. Bagolini B, Tamburrelli C, Dickmann A, Colosimo C. Convergent strabismus in high myopic patients. *Doc Ophthalmol.* 1990;74: 309–320.
35. Poukens V, Glasgow BL, Demer JL. Nonvascular contractile cells in sclera and choroid of human and monkey. *Invest Ophthalmol Vis Sci.* 1998;39:1765–1774.
36. Siegel LM, De Salles N, Rosenbaum AL, Demer JL. Magnetic resonance imaging features of two cases of acquired Brown's syndrome. *Strabismus.* 1998;6:19–29.

37. Sprunger DT, von NG, Helveston EM. Surgical results in Brown syndrome. *J Pediatr Ophthalmol Strabismus.* 1991;28:164–167.
38. Santiago AP, Rosenbaum AL. Grave complications after superior oblique tenotomy or tenectomy for Brown syndrome. *J Am Assoc Pediatr Ophthalmol Strabismus.* 1997;1:8–15.
39. Crawford JS, Orton RB, Labow-Daily L. Late results of superior oblique muscle tenotomy in true Brown syndrome. *Am J Ophthalmol.* 1980;89:824–829.
40. Velez FG, Demer JL. Rectus extraocular muscle (EOM) pulley instability: a cause of incomitant strabismus. *Abstracts of XIV Latin-American Congress on Strabismus.* 2000;11.
41. Dietz HC, Pyeritz RE. Mutations in the human gene for fibrillin-1 (FBN1) in the Marfan syndrome and related disorders. *Hum Mol Gen.* 1995;4:1799–1809.
42. Tynan K, Comeau K, Pearson M, et al. Mutation screening of complete fibrillin-1 coding sequence: report of five new mutations, including two in 8-cysteine domains. *Hum Mol Gen.* 1993; 2:1813–1821.
43. Wheatley HM, Traboulsi EI, Flowers BE. et al. Immunohistochemical localization of fibrillin in human ocular tissues: relevance to the Marfan syndrome. *Arch Ophthalmol.* 1995;113: 103–109.
44. Potter KA, Hoffman Y, Sakai L. et al. Abnormal fibrillin metabolism in bovine Marfan syndrome. *Am J Pathol.* 1993;142:803–810.
45. Cross HE, Jensen AD. Ocular manifestations in the Marfan syndrome and homocystinuria. *Am J Ophthalmol.* 1973;75:405–420.
46. Izquierdo NJ, Traboulsi EI, Enger C, Maumenee IH. Strabismus in the Marfan syndrome. *Am J Ophthalmol.* 1994;117:632–635.
47. Hanssen E, Franc S, Garrone R. Fibrillin-rich microfibrils: structural modifications during ageing in normal human zonule. *J Submicrosc Cytol Pathol.* 1998;30:365–369.